WARSAW UNIVERSITY OF TECHNOLOGY Index 351733
FACULTY OF CIVIL ENGINEERING
COMMITTEE FOR CIVIL AND WATER ENGINEERING
POLISH ACADEMY OF SCIENCES ISSN 1230-2945

DOI: 10.24425/ace.2021.138512

ARCHIVES OF CIVIL ENGINEERING

Vol. LXVII ISSUE 4 2021

pp. 469 –486

Research paper

Optimal design of archgrids: the second-order cone programming perspective

Grzegorz Dzierżanowski[1], Krzysztof Hetmański[2]

Abstract: This paper regards the minimum weight problem of spatial systems, known in the literature as Rozvany–Prager archgrids. Their architectural role is to transmit a load of fixed intensity to the line of supports located at the boundary of a given plane domain. The system consists of arches spaced apart from one another, hence the mechanics of such a system is that of a gridwork shell and not a shell continuum. Mathematically, description of an archgrid falls into the class of Michell frames. Therefore, in our approach, we make use of the plastic design paradigm – it states that optimal bar structure is at the verge of plastic failure, with bars uniformly stressed to the limit value in compression, or tension. In the case of archgrid optimization, only compression is allowed and this limitation introduces an additional design constraint. The main goal of this paper is computational, thus the general variational framework of the optimization problem is reformulated in the discrete setting, involving the methods of linear algebra. Numerics of the discrete approach to Rozvany–Prager archgrids is considered from the novel perspective based on second-order cone programming (SOCP). Procedures used for solving the examples are coded in MATLAB combined with MOSEK optimization toolbox for SOCP routines.

Keywords: minimum volume structures, optimal archgrids, Rozvany–Prager archgrids, cone programming

[1]DSc., PhD., Eng., Warsaw University of Technology, Faculty of Civil Engineering, al. Armii Ludowej 16, 00-637 Warsaw, Poland, e-mail: gd@il.pw.edu.pl, ORCID: 0000-0003-1676-0875

[2]PhD., Eng., Warsaw University of Technology, Faculty of Civil Engineering, al. Armii Ludowej 16, 00-637 Warsaw, Poland. Deceased 4 April 2020

1. Introduction

1.1. The Rozvany–Prager archgrids

The scientific interest in optimal design of archgrids has been initiated in the late 1970s by G.I.N. Rozvany and W. Prager, [11]. They put forward a problem of minimizing the weight (or, equivalently, volume) of a spatial structure composed of arches spanning a given plane domain and transmitting a load of fixed intensity to the line of supports located at the boundary of that domain. Such an arch system is best visualized as a ribbed vault (arch-like roof) over the domain, with single ribs (arches) spaced apart from one another. Architecturally speaking, the vault has a form of a dense grid of curved bars pinned at both ends. Therefore, the mechanics of the roof is that of a gridwork shell and not a shell continuum. Following this lead, in our paper we use the terms *Rozvany–Prager archgrid* to emphasize the specific arch-like pattern of the vault.

The minimum volume problem for archgrids belongs to the broad topic of structural topology optimization. More specifically, *Rozvany–Prager archgrids* can be identified as a particular class within *Prager structures*, which, in turn, form the subcategory of *Michell frames*, or, in set notation:

$$\textit{Rozvany–Prager archgrids} \subseteq \textit{Prager structures} \subseteq \textit{Michell frames}$$

Various aspects of Prager structures and Rozvany–Prager archgrids are covered in the early works, [10, 12, 13, 17], while the most recent and comprehensive study of the most general (Michell) category of optimal structures can be found in [9].

In order to highlight the differences among the three concepts in structural topology optimization, we recall the *plastic design paradigm*. It is one out of two Michell–Hemp conditions determining a structure of minimum volume of material, [7]. The paradigm is static by nature and states that stresses in the material used for the construction of the optimally designed structure reach the elastic threshold. We say, that the entire Michell frame is at the verge of plastic failure, with bars uniformly stressed to the limit value, say σ_C, if the bar is in compression, or $-\sigma_T$ if the bar is in tension (compression stress is assumed positive for the convenience of further discussion). This, in turn, involves an implicit requirement that bars in the optimally designed frame are bending- and shear-free. In other words, external load is carried by arches subjected to axial stress resultants only.

The plastic design paradigm applies also to Prager structures and Rozvany–Prager archgrids, with an additional assumption that stresses are univalent – compressive or tensile – in the entire system. Since in this work we focus on bar structures that are entirely in compression, then we fix $\sigma_C = \sigma_0 > 0$ and $\sigma_T = 0$. The opposite assumption paves way to optimal design of tension-only cable networks, but we skip the discussion of this topic, because it is a matter of a straightforward modification of the results presented in the remainder of the paper.

The other Michell–Hemp condition is of kinematic type. We do not recall it here, as it does not provide new arguments that are helpful in explaining the differences among the Michell, Prager, and Rozvany–Prager notions of optimality.

1.2. Motivation for the present study

Michell–Hemp conditions (both the static and kinematic one) are bar-wise. Computational algorithms enforce these conditions for single straight bars, which are basic members of large-scale frames, see e.g. [6, 15] for various numeric techniques appropriate in this context. Such a strategy leads to optimal designs in the sense of Michell and Prager. Rozvany–Prager archgrids require different design procedures, with the primary focus shifted from single bars towards plane arches, represented in the discrete approach by arch-shaped sequences of straight bars, and pinned at both ends. Thus, Michell–Hemp criteria need to be properly reformulated, so that they apply to multi-bar curvilinear grid elements of this type. It turns out, however, that adjusting the Michell structure-oriented numerical algorithms to the specifics of Rozvany–Prager archgrids is not straightforward. By the above, the main difficulty is in redefining the optimality criteria from bar-wise (Michell–Hemp) to arch-wise (Rozvany–Prager).

This observation justifies the research effort, whose central interest is in the criteria for the optimality of spatial systems with single plane arches understood as basic members. Rozvany and Prager, [11], introduced *the mean squared slope condition*, that is a formula characterizing the optimality of elevation functions of the plane arch, see Eq. (2.2). They also outlined a variational attitude toward minimum volume design of archgrids with orthogonal layout of arches supported at the boundary of the roofed domain. Mathematical structure of the right-angled archgrid problem was formalized in [4], see also [8], thus paving way for numerical procedures in the continuous and discrete setting, [3, 5]. The authors of [16], argued that if the line of supports coincides with the boundary of roofed domain then the theory of Rozvany–Prager archgrids extends beyond the case of orthogonal layout of members, i.e. it embraces arch systems with elements running in arbitrary directions.

In our paper, the numerics corresponding to the discrete approach to Rozvany–Prager archgrids is further developed from the second-order cone programming (SOCP) perspective. Numerical procedures used for solving the examples in this paper has been coded in MATLAB, [18], combined with the third-party MOSEK optimization toolbox for SOCP routines, [19]. Computational algorithm used in this new outlook proves to be more efficient in terms of CPU-time, than the routine used so far. This, in turn, allows for analyzing the structures with a very large ($\sim 10^6$) number of arches. Results obtained for such an extremely populated archgrids may well serve to hint the research aimed at optimization problems posed in the continuous setting, but they clearly exceed the rational needs of civil engineering industry.

The latter naturally comes along with a call for methods transforming optimal layouts to realistic constructions satisfying the requirements imposed by the building codes and standards. Such a rationalization usually involves coarsening the pattern of structural members, strengthening selected areas of the design to avoid stress localization, resizing the members prone to buckling, etc. An example of a computer algorithm replacing the Michell-type structure with a ready-to-fabricate prototype is presented in [14], while other industrial applications of the theoretically predicted solutions are discussed in [8, 9]. Solutions related to this study for archgrids with various coarseness of members are compared in the examples, see Section 3.

2. The minimum volume problem

2.1. Outline of the variational formulation

Since the numerical study in this paper is based on the variational formulation of the Rozvany–Prager problem, we briefly outline the latter below. For definiteness, we denote the roofed domain by Ω and suppose that Γ stands for the line of supports for arches. In this research, we assume that Γ coincides with the boundary of Ω, and we write $\Omega_0 = \Omega \cup \Gamma$. We also let (x, y) represent the Cartesian coordinates in Ω_0, and write $q = q(x, y)$ for the intensity of the external load acting on the archgrid.

Next, we express the assumptions of the Rozvany–Prager theory:

i) a single arch – precisely, its neutral axis – belongs to a plane extending perpendicularly from Ω;

ii) axes of all arches are located on a single surface, say $v = v(x, y)$, such that $v(x, y) = 0$ for $(x, y) \in \Gamma$; function v is referred to as *archgrid elevation function*;

iii) load q also acts perpendicular to Ω – i.e. along the z-axis in the 3-dimensional Cartesian system (x, y, z); the position of q with respect to the z-direction is determined by function v.

In light of the discussion in the previous Section, planes mentioned in *i*) above are not constrained to run in two orthogonal directions. To account for the variety of arch orientations in a large-scale archgrid, we suppose that, see Fig. 1b:

– the archgrid consists of k arches;

– $0 \le \psi_K \le 2\pi$ is the orientation angle of the plane, say π_K, extending perpendicularly from Ω and containing the K-th arch ($K = 1, \ldots, k$); the line of intersection of π_K and Ω determines the K-th arch axis x_K inclined on the plane Ω by angle ψ_K to the reference x-axis;

– load q is distributed between the arches in such a way that the arch loads, q_K, satisfy

$$\int_\Omega q(x, y)v(x, y)\,\mathrm{d}x\,\mathrm{d}y = \sum_{K=1}^{k} \int_0^{L_K} q_K(x_K)v_K(x_K)\,\mathrm{d}x_K \tag{2.1}$$

where: L_K denotes the span of the K-th arch, v_K and v are functions, satisfying $v_K(x_K(x, y)) = v(x, y)$ for $(x, y) \in \pi_K \cap \Omega_0$, see *ii*) in the previous page;

– the K-th arch is optimal if the elevation function v_K satisfies the condition known in the literature as *the mean squared slope condition* by Rozvany and Prager:

$$\left(\int_0^{L_K} (s_K(x_K))^2 \,\mathrm{d}x_K \right)^{\frac{1}{2}} = \sqrt{L_K}, \quad s_K = \frac{\mathrm{d}v_K}{\mathrm{d}x_K} \tag{2.2}$$

Expression on the left hand side of the first Eq. (2.2) defines the norm in the space of square-integrable functions (L^2 space). In the remainder of this Section, we use the notation $\|\cdot\|_2$ to denote this norm.

The *primary optimization problem*, (P_1), with the primary variable $v \in \mathcal{V}$, and the *dual optimization problem*, (P_2), with the dual variable $\{Q_1 \dots Q_K\} \in \Sigma$, are respectively given by

$$(P_1)\quad \left| \begin{array}{l} Z_1 = \sup\left\{ \displaystyle\int_\Omega qv \,\mathrm{d}\Omega \;\middle|\; v \in V \right\} \\ \text{where:} \\ \mathcal{V} = \left\{ v \;\middle|\; \begin{array}{ll} v(x,y), \quad v(x,xy) = 0, & \text{for } (x,y) \in \Gamma \\ \|sk\|_2 \le \sqrt{L_k}, \quad s_k(x_k) = \dfrac{\mathrm{d}v_k}{\mathrm{d}x_k}(x_k(x,y)), & \text{for } (x,y) \in \pi_k \cap \Omega_0 \text{ and } K = 1,\dots,k \end{array} \right\} \end{array} \right.$$

$$(P_2)\quad \left| \begin{array}{l} Z_2 = \inf\left\{ \displaystyle\sum_{K=1}^{k} \sqrt{L_K}\, \|Q_K\|_2 \;\middle|\; (Q_1,\dots,Q_k) \in \Sigma \right\} \\ \text{where:} \\ \Sigma = \left\{ (Q_1,\dots,Q_k) \;\middle|\; \displaystyle\sum_{K=1}^{k} \int_0^{L_K} Q_K(x_K) \frac{\mathrm{d}\overline{v}_K}{\mathrm{d}x_k}(x_k)\mathrm{d}x_k = \int_\Omega \text{ for any } \overline{v} \text{ with } \overline{v} = 0 \text{ at } \Gamma \right\} \end{array} \right.$$

Functions Q_K have clear mechanical interpretation following from the equilibrium equations concerning a single arch subjected to the load q_K and axial forces N_K only. Full derivation of the formulae is dropped, as this is a classical topic in the theory of bar structures. The equations read

$$Q_K(x_K) = N_K \sin\phi_K(x_K) = H_K \frac{\mathrm{d}v_K}{\mathrm{d}x_K}(x_K), \qquad \frac{\mathrm{d}Q_K}{\mathrm{d}x_K} + q_K = 0, \quad \text{for } K = 1,\dots,k \tag{2.3}$$

where: H_K denotes the horizontal thrust at pinned supports of an arch, φ_K is an angle of slope of v_K, see Fig. 1c).

Assuming that v_{opt} and $(Q_{1,\text{opt}}, \dots, Q_{k,\text{opt}})$ stand for the solutions to (P_1) and (P_2) respectively, one may show, using also the Eq. (2.3) above, that $Z_1 = Z_2 = Z$. We skip the proof of this fact, referring the reader to [4] and literature cited therein. Here, we only mention that the optimal volume of an archgrid is given by

$$V_{\text{opt}} = \frac{2}{\sigma_0} Z \tag{2.4}$$

The formula for optimal cross-section area reads,

$$A_{K,\text{opt}}(x_K) = \frac{N_{K,\text{opt}}(x_K)}{\sigma_0} = \frac{1}{\sigma_0}\left[\left(Q_{K,\text{opt}}(x_K)\right)^2 + \frac{\left(\left\|Q_{K,\text{opt}}\right\|_2\right)^2}{L_K} \right]^{\frac{1}{2}}. \tag{2.5}$$

The expression for optimal horizontal thrust takes the form

$$H_{K,\text{opt}} = \frac{\left\|Q_{K,\text{opt}}\right\|_2}{\sqrt{L_K}} \tag{2.6}$$

Applying the latter in the first Eq. (2.3), and calculating the $\|\cdot\|_2$ norm at both sides of thus obtained formula, we finally arrive at the mean squared slope condition, see Eq. (2.2).

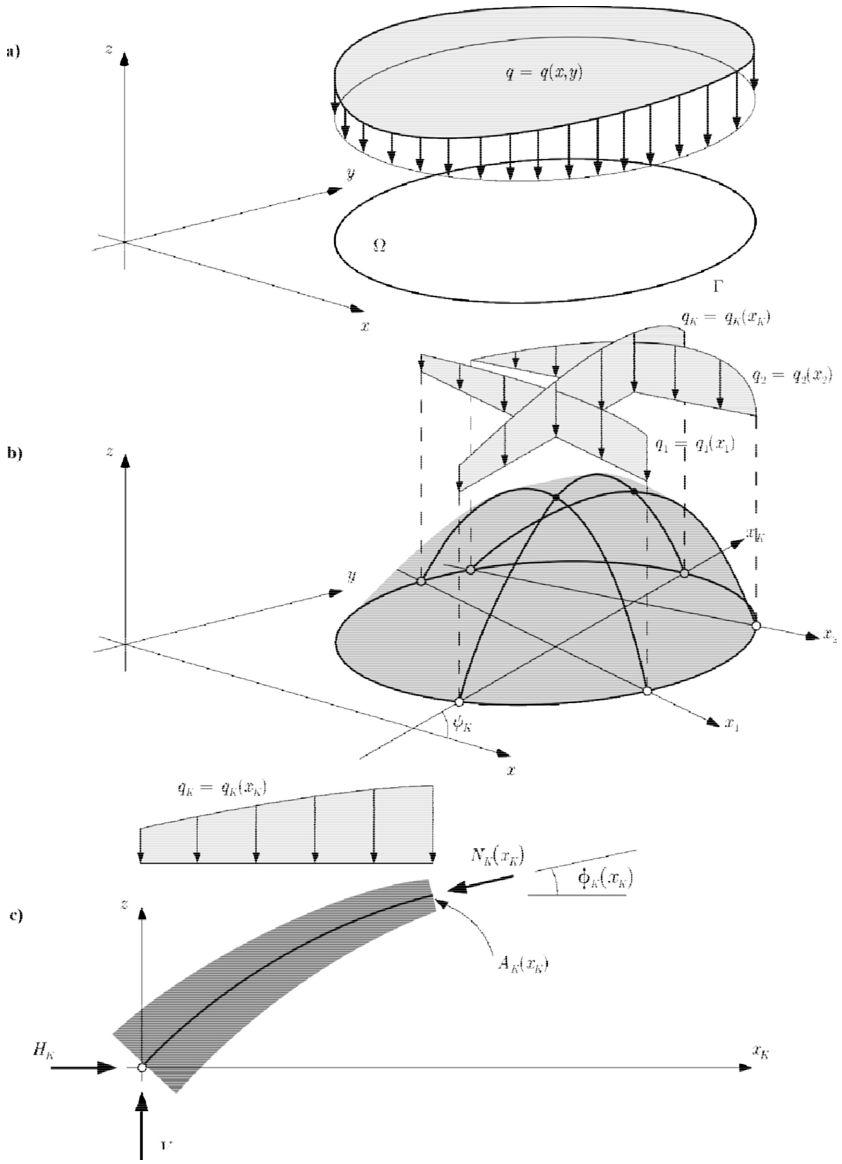

Fig. 1. a) load $q = q(x, y)$ over domain Ω, whose boundary coincides with line of supports Γ, b) archgrid elevation function $v = v(x, y)$ – shown in transparent grey, single arch elevation functions $v_1, v_2 \ldots, v_K, \ldots$ – shown as thick black lines, and arch loads $q_1, q_2 \ldots, q_K \ldots$, c) arch segment subjected to load q_K balanced by reaction components V_K and H_K (horizontal thrust) and axial stress resultant $N_K(x_K)$; arch cross-section area, $A_K(x_K)$, varies along the arch x_K-axis according to the formula

$$A_K(x_K) \cdot \sigma_0 = N_K\ (x_K)$$

2.2. The second-order cone programming approach

The main objective of this paper is computational, hence the need for reformulation of expressions from Sec. 2.1 in terms of linear algebra. We choose a mesh of n nodes in Ω_0 at which the elevation of surface v is sampled, and we write $\boldsymbol{u} \in \mathbb{R}^n$ for the vector of elevations – measured in meters – and $\boldsymbol{f} \in \mathbb{R}^n$ for the load vector – measured in newtons. Vector $\boldsymbol{f}$ satisfies the counterpart of Eq. (2.1),

$$\int_{\Omega} q(x,y)v(x,y)\,\mathrm{d}x\,\mathrm{d}y = \sum_{N=1}^{n} f_N u_N = \boldsymbol{f}^T\boldsymbol{u}$$

where: symbol T denotes the transposition of a vector.

Now, we consider an arbitrary K-th arch ($K = 1, \ldots, k$). Its elevation function v_K is sampled at nodes located along the x_K-axis (boundary nodes included). The number of sampling points, $p(K)$, may differ for $K = 1, \ldots, k$, as any such number depends on the placement of the given arch in the archgrid. Thus, arch elevation vectors $\boldsymbol{u}_K \in \mathbb{R}^{p(K)}$ contains different number of components, but each vector $\boldsymbol{u}_1, \ldots \boldsymbol{u}_k$ is a subvector of $\boldsymbol{u}$, and such that $u_K^1 = u_K^{p(K)} = 0$ (elevation of the points located at the boundary Γ is equal to 0). In the discrete approach, the K-th arch is represented by a collection of straight bars located on the plane π_K; the number of bars in this collection equals $m_K = p(K) - 1$, see Fig. 2.

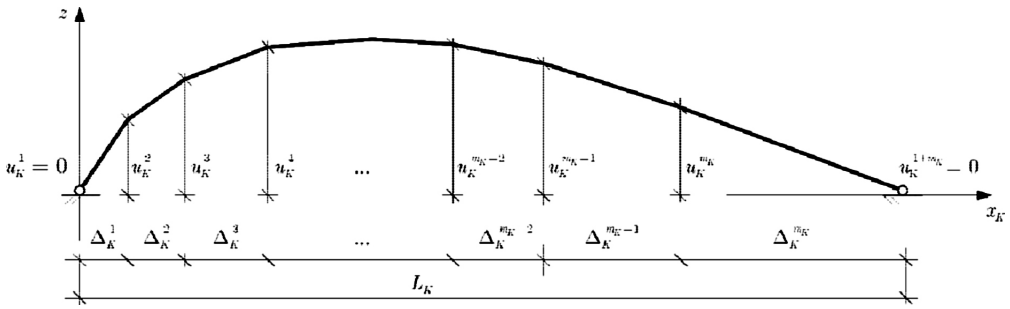

Fig. 2. K-th arch composed of m_K straight bars linking the sample points at the arch elevation function v_K

Next, we reformulate the mean squared slope condition of Rozvany and Prager in Eq. (2.2):

$$\|\boldsymbol{t}_K\|_2 = \sqrt{L_K}, \quad \|\boldsymbol{t}_K\|_2 = \sqrt{\left(t_K^1\right)^2 + \left(t_K^2\right)^2 + \ldots + \left(t_K^{m_K}\right)^2}, \tag{2.7}$$

where: $\|\cdot\|_2$ now stands for the Euclidean norm in a finite-dimensional real space.

We emphasize that the first Eq. (2.7) represents the discretized form of the entire integral (not just the integrand) on the left hand side of the first Eq. (2.2). For this, the components of vector $\boldsymbol{t}_K \in \mathbb{R}^{m_K}$ ($K = 1, \ldots, k$) are defined as a forward finite differences of the elevation function v_K (slope of v_K) multiplied by the square root of the spacing.

Explicitly,

$$\boldsymbol{t}_K = \begin{bmatrix} t_K^1 \\ t_K^2 \\ \vdots \\ t_K^{m_K} \end{bmatrix} = \begin{bmatrix} \left(\dfrac{u_K^2 - u_K^1}{\Delta_K^1}\right) \cdot \sqrt{\Delta_K^1} \\ \left(\dfrac{u_K^3 - u_K^2}{\Delta_K^2}\right) \cdot \sqrt{\Delta_K^2} \\ \vdots \\ \left(\dfrac{u_K^{1+m_K} - u_K^{m_K}}{\Delta_K^{m_K}}\right) \cdot \sqrt{\Delta_K^{m_K}} \end{bmatrix} \tag{2.8}$$

where: $\Delta_K^1, \Delta_K^2, \ldots, \Delta_K^{m_K}$ is the sequence of spacings between successive sampling points along the x_K-axis.

Similarly to $\boldsymbol{u}_1, \ldots, \boldsymbol{u}_k$, also the lengths of $\boldsymbol{t}_1, \ldots, \boldsymbol{t}_k$ may not be equal. The span of the K-th arch is

$$L_K = \Delta_K^1 + \Delta_K^2 + \ldots + \Delta_K^{m_K}$$

and we consider vector $\boldsymbol{l} \in \mathbb{R}^k$,

$$\boldsymbol{l} = \begin{bmatrix} l_1 \\ \vdots \\ l_K \end{bmatrix} = \begin{bmatrix} \sqrt{L_1} \\ \vdots \\ \sqrt{L_K} \end{bmatrix}$$

Vectors $\boldsymbol{u}$ and $\boldsymbol{t}_1, \ldots, \boldsymbol{t}_k$ are constrained by Eq. (2.8). This is accounted for by introducing the matrices $\boldsymbol{B}_K \in \mathbb{R}^{m_K \times n}$, such that

$$\boldsymbol{B}_K \boldsymbol{u} = \boldsymbol{t}_K \tag{2.9}$$

and we note that matrix $\boldsymbol{B}_K$ $(K = 1, \ldots, k)$ takes the place of the differential operation in Eq. (2.2). We note, however, that the unit of components in vector $\boldsymbol{t}_K$ in Eq. (2.8) is the $(\text{meter})^{1/2}$ in contrast to Eq. (2.2), where the values of s_K are no unit numbers. We therefore conclude, that the components of matrices $\boldsymbol{B}_K$ are measured in $1/(\text{meter})^{1/2}$. From the mathematical standpoint, Eqs. (2.7) and (2.9) define k second-order (quadratic) cones; the K-th cone, $\boldsymbol{C}_K \in \mathbb{R}^{1+m_K}$ $(K = 1, \ldots, k)$, is given by

$$\boldsymbol{C}_K = \left\{ \left(\sqrt{L_K}, \boldsymbol{B}_K \boldsymbol{u}\right) \,\middle|\, \|\boldsymbol{B}_K \boldsymbol{u}\|_2 \leq \sqrt{L_K} \right\} \tag{2.10}$$

In what follows, we refer to $\boldsymbol{C}_K$ as the primal cone.

With this, the discrete counterpart of the primal optimization problem (P_1) reads

$$(\hat{P}_1) \quad \left| \begin{array}{l} \hat{Z}_1 = \max \left\{ \boldsymbol{f}^T \boldsymbol{u} \,|\, \boldsymbol{u} \in U \right\} \\ \text{where:} \\ \mathcal{U} = \left\{ \boldsymbol{u} \,\middle|\, \begin{array}{l} \boldsymbol{u} \in \mathbb{R}^n \ \text{ and } \ u_N = 0 \ \text{ if } N\text{-th node is placed at } \Gamma; \\ \left(\sqrt{L_k}, \boldsymbol{B}_K \boldsymbol{u}\right) \in \boldsymbol{C}, \ \text{ for all } \ K = 1, \ldots, k \end{array} \right\} \end{array} \right.$$

Dual optimization problem is typically derived by the use of Lagrange multiplier technique. We recall it here with a goal to determine the dual variables $(\boldsymbol{T}_1, \ldots, \boldsymbol{T}_k)$, being the discrete counterparts of $(Q_1, \ldots, Q_k)$, and, consequently, to calculate of the cross-section area vectors $\boldsymbol{A}_1, \ldots, \boldsymbol{A}_k$. To this end, we first notice, that by the Cauchy–Schwarz inequality,

$$\boldsymbol{h}^T (\boldsymbol{B}_K \boldsymbol{u}) \leq \|\boldsymbol{h}\|_2 \, \|\boldsymbol{B}_K \boldsymbol{u}\|_2 \quad \text{for all } \boldsymbol{h} \in \mathbb{R}^{m_K}$$

This, specified for $\boldsymbol{h}$ with $\|\boldsymbol{h}\|_2 = 1$, and combined with the set builder condition in Eq. (2.10), gives

$$\sqrt{L_K} - \boldsymbol{h}^T (\boldsymbol{B}_K \boldsymbol{u}) \geq 0 \quad \text{for all } \boldsymbol{h} \in \mathbb{R}^{m_K} \quad \text{such that } \|\boldsymbol{h}\|_2 = 1$$

Next, we define the Lagrange function associated with $(\hat{P}_1)$. Namely, we write

$$\begin{aligned} \mathcal{L}(\boldsymbol{u}, \boldsymbol{\lambda}, \boldsymbol{T}_1, \ldots, \boldsymbol{T}_k) &= \boldsymbol{f}^T \boldsymbol{u} + \sum_{K=1}^{k} \lambda_K \left(\sqrt{L_K} - \boldsymbol{h}_T (\boldsymbol{B}_k \boldsymbol{u}) \right) \\ &= \boldsymbol{f}^T \boldsymbol{u} + \sum_{K=1}^{k} \left(\lambda_K \sqrt{L_K} - (\boldsymbol{T}_k)^T (\boldsymbol{B}_k \boldsymbol{u}) \right) \end{aligned} \tag{2.11}$$

where: $\boldsymbol{\lambda} \in \mathbb{R}^k$, $\lambda_K > 0$, and $\lambda_K \boldsymbol{h} = \boldsymbol{T}_K \in \mathbb{R}^{m_K}$ $(K = 1, \ldots, k)$ are the Lagrange multipliers (dual variables).

Pairs $(\lambda_K, \boldsymbol{T}_K)$ belong to dual cones $\boldsymbol{C}_K^*$ $(K = 1, \ldots, k)$ and since the primal cones, $\boldsymbol{C}_K$, defined in Eq. (2.10), are quadratic, then $\boldsymbol{C}_K^* = \boldsymbol{C}_K$, see [2]. Therefore, from Eq. (2.10) we conclude that

$$\|\boldsymbol{T}_K\|_2 \leq \lambda_K \quad \text{for all } K = 1, \ldots, k \tag{2.12}$$

Moreover, the sum in Eq. (2.11) is non-negative. Hence,

$$\boldsymbol{f}^T \boldsymbol{u} \leq \mathcal{L}\,(\mathbf{u},\ \lambda, \boldsymbol{T}_1, \ldots, \boldsymbol{T}_k)$$

for all $\boldsymbol{u}$ admissible in $(\hat{P}_1)$. Maximizing both sides of this inequality over $\boldsymbol{u} \in U$, we get

$$\begin{aligned} \hat{Z} \leq g(\boldsymbol{\lambda}, \boldsymbol{T}_1, \ldots, \boldsymbol{T}_k) &= \sum_{K=1}^{k} \lambda_K \sqrt{L_K} + \max_{\boldsymbol{u}} \boldsymbol{u}^T \left(\boldsymbol{f} - \sum_{K=1}^{k} (\boldsymbol{B}_K)^T \boldsymbol{T}_K \right) \\ &= \sum_{K=1}^{k} \lambda_K \sqrt{L_K} + \begin{cases} 0 & \text{if } \displaystyle\sum_{K=1}^{k} (\boldsymbol{B}_K)^T \boldsymbol{T}_K = \boldsymbol{f} \\ +\infty & \text{otherwise} \end{cases} \end{aligned} \tag{2.13}$$

where: $g(\boldsymbol{\lambda}, \boldsymbol{T}_1, \ldots, \boldsymbol{T}_k)$ is the dual function of the Lagrangian $\mathcal{L}$, and the constraint on $(\boldsymbol{T}_1, \ldots, \boldsymbol{T}_k)$ replaces the second expression in Eq. (2.3).

Function g is now minimized over $\boldsymbol{\lambda}$. This, by making use of Ineq. (2.12), leads to $\lambda_K = \|\boldsymbol{T}_K\|_2$ for all $K = 1, \ldots, k$. Consequently, $\hat{Z}_1 \leq \hat{Z}_2$, where $\hat{Z}_2$ is the solution to the dual

optimization problem in the discrete setting

$$(\hat{P}_2)\quad \left|\begin{array}{l} \hat{Z}_2 = \min\left\{\displaystyle\sum_{K=1}^{k}\sqrt{L_K}\,\|\boldsymbol{T}_K\|_2 \,|\,(\boldsymbol{T}_1,\ldots,\boldsymbol{T}_k)\in\Phi\right\} \\ \text{where:} \\ \Phi = \left\{(\boldsymbol{T}_1,\ldots,\boldsymbol{T}_k)\;\middle|\; \begin{array}{l}\boldsymbol{T}_k\in\mathbb{R}^n \text{ for all } u_N = 0 \text{ if } N\text{-th node is placed at } \Gamma; \\ \displaystyle\sum_{K=1}^{k}(\boldsymbol{B}_K)^T\boldsymbol{T}_K = \boldsymbol{f}\end{array}\right\}\end{array}\right.$$

and, similarly to Sec. 2.1, we have $\hat{Z}_1 \le \hat{Z}_2 = \hat{Z}$. Explanation of this fact is postponed to Sec. 2.3.

Optimal volume of the archgrid, V_{opt}, follows from Eq. (2.4). Moreover, having $(\hat{P}_2)$ solved, one may calculate optimal horizontal thrust $H_{K,\text{opt}}$ for all $K = 1,\ldots,k$,

$$H_{K,\text{opt}} = \frac{\left\|\boldsymbol{T}_{K,\text{opt}}\right\|_2}{\sqrt{L_K}} \tag{2.14}$$

as well as optimal cross-section areas, now represented by vectors $\boldsymbol{A}_{K,\text{opt}}$ for $K-$th arch,

$$\boldsymbol{A}_{K,\text{opt}} = \begin{bmatrix} A^1_{K,\text{opt}} \\ A^2_{K,\text{opt}} \\ \vdots \\ A^{m_K}_{K,\text{opt}}\end{bmatrix} \quad \text{with } A^1_{K,\text{opt}} = \frac{1}{\sigma_0}\left[\left(\frac{T^1_{K,\text{opt}}}{\sqrt{\Delta^1_K}}\right)^2 + \frac{\left(\left\|\boldsymbol{T}_{K,\text{opt}}\right\|_2\right)^2}{L_K}\right]^{\frac{1}{2}}, \text{ etc.}$$

In light of the remarks on units of the components of vector $\boldsymbol{f}$ and matrices $\boldsymbol{B}_K$, we conclude that the elements of $\boldsymbol{T}_{K,\text{opt}}$ $(K = 1\ldots,k)$ are measured in newton $\times$ (meter)$^{1/2}$. Therefore, to get the proper discrete counterpart of Eq. (2.5), we define the vector

$$\begin{bmatrix} \dfrac{T^1_{K,\text{opt}}}{\sqrt{\Delta^1_K}} \\ \vdots \\ \dfrac{T^{m_K}_{K,\text{opt}}}{\sqrt{\Delta^{m_K}_K}}\end{bmatrix} \in \mathbb{R}^{m_K}$$

representing the values of function $Q_{K,\text{opt}}$, measured in newtons. Note that $\|\boldsymbol{T}_{K,\text{opt}}\|_2$ in the calculations of $\boldsymbol{A}_{K,\text{opt}}$ and $\|Q_{K,\text{opt}}\|_2$ in Eq. (2.5) are both measured in newton $\times$ (meter)$^{1/2}$.

2.3. Discussion of the optimal solution

From the duality theory, it follows that $\hat{Z}_1 \le \hat{Z}_2$, and below we show that, factually, $\hat{Z}_1 = \hat{Z}_2$. Our argument rests on the assumption that the set Φ in $(\hat{P}_2)$ is not empty, i.e. for fixed load

vector $\boldsymbol{f}$, there exist at least one collection $(\boldsymbol{T}_1, \ldots, \boldsymbol{T}_k)$ for which the set builder condition makes sense. With this, we write

$$\hat{Z}_2 = \min_{\boldsymbol{\lambda}, \boldsymbol{T}_1, \ldots, \boldsymbol{T}_k} \mathcal{L}(\boldsymbol{u}, \boldsymbol{\lambda}, \boldsymbol{T}_1, \ldots, \boldsymbol{T}_k) = \mathcal{L}\left(\boldsymbol{u}, \boldsymbol{\lambda}_{\text{opt}}, \boldsymbol{T}_{1,\text{opt}}, \ldots, \boldsymbol{T}_{k,\text{opt}}\right) \tag{2.15}$$

where: $\boldsymbol{u}$ is arbitrary.

Next, we notice that

$$\begin{aligned} \hat{Z}_1 &= \max_{\boldsymbol{u}} \mathcal{L}\left(\boldsymbol{u}, \boldsymbol{\lambda}_{\text{opt}}, \boldsymbol{T}_{1,\text{opt}} \ldots, \boldsymbol{T}_{k,\text{opt}}\right) \\ &= \max_{\boldsymbol{u}} \left\{ \boldsymbol{f}^T \boldsymbol{u} + \sum_{K=1}^{k} \alpha_K \sum_{K=1}^{k} \left(\sqrt{L_K} \|\boldsymbol{T}_{K,\text{opt}}\|_2 - \left(\boldsymbol{T}_{K,\text{opt}}^T\right) (\boldsymbol{B}_K \boldsymbol{u}) \right) \right\} \end{aligned} \tag{2.16}$$

and, for fixed $\boldsymbol{u}$, the sum involved in Eq. (2.16) achieves its maximum value if

$$\boldsymbol{T}_{K,\text{opt}} = \alpha_K \boldsymbol{B}_K \boldsymbol{u} \quad \text{for all} \quad K = 1, \ldots, k \tag{2.17}$$

where: $\alpha_K \geq 0$.

Consequently, the problem

$$\begin{aligned} \hat{Z} &= \max_{\boldsymbol{u}} \left\{ \boldsymbol{f}^T \boldsymbol{u} + \sum_{K=1}^{k} \alpha_K \|\boldsymbol{B}_K \boldsymbol{u}\|_2 \sum_{K=1}^{k} \left(\sqrt{L_K} - \|\boldsymbol{B}_K \boldsymbol{u}\|_2 \right) \right\} \\ &= \max_{\boldsymbol{u}} \boldsymbol{f}^T \boldsymbol{u} + \begin{cases} 0 & \text{if} \quad \left(\sqrt{L_K} \boldsymbol{B}_K \boldsymbol{u}\right) = \boldsymbol{C}_K \\ +\infty & \text{otherwise} \end{cases} \end{aligned}$$

coincides with $(\hat{P}_1)$. Thus

$$\hat{Z}_1 = \boldsymbol{f}^T \boldsymbol{u}_{\text{opt}} = \mathcal{L}\left(\boldsymbol{u}_{\text{opt}}, \lambda_{\text{opt}}, \boldsymbol{T}_{1,\text{opt}}, \ldots, \boldsymbol{T}_{k,\text{opt}}\right) = \hat{Z}_2$$

which follows from Eq. (2.15) with $\boldsymbol{u} = \boldsymbol{u}_{\text{opt}}$.

From Eqs. (2.9) and (2.17),

$$\boldsymbol{T}_{K,\text{opt}} = \alpha_K \boldsymbol{t}_{K,\text{opt}} \quad \text{for all } K = 1, \ldots, k \tag{2.18}$$

Hence, if $\alpha_K = \|\boldsymbol{T}_{K,\text{opt}}\|_2 / \sqrt{L_K} = H_{K,\text{opt}}$, see Eq. (2.14), then Eq. (2.18) becomes

$$\boldsymbol{T}_{K,\text{opt}} = H_{K,\text{opt}} \boldsymbol{t}_{K,\text{opt}} \quad \text{for all} \quad K = 1, \ldots, k$$

being the discrete counterpart of the first Eq. (2.3). Also, recall that $\boldsymbol{T}_{K,\text{opt}} = \lambda_{K,\text{opt}} \boldsymbol{h}$ for arbitrary $\boldsymbol{h}$ with $\|\boldsymbol{h}\|_2 = 1$, see Eq. (2.11), and $\lambda_{K,\text{opt}} = \|\boldsymbol{T}_{K,\text{opt}}\|_2$. Thus,

$$\boldsymbol{h} = \frac{1}{\sqrt{L_K}} \boldsymbol{t}_{K,\text{opt}} \quad \text{for all} \quad K = 1, \ldots, k$$

and

$$\left\| \boldsymbol{t}_{K,\text{opt}} \right\|_2 = \sqrt{L_K} \quad \text{for all } K = 1, \ldots, k$$

which again provides the discrete variant of the Rozvany–Prager condition, see Eq. (2.7).

3. Numerical examples

Numerical simulations in all examples presented in the paper were performed on a laptop computer equipped with the Intel Core i7-4600U CPU @ 2.10 GHz (2 processors), 8 GB RAM, 64-bit Windows 10 Pro, and MathWorks MATLAB R2021a with MOSEK optimization toolbox version 9.2.

For conic optimization problems, an interior-point type optimizer based on the so-called homogeneous and self-dual algorithm is available in MOSEK, see [19] for the documentation containing technical details on this algorithm. The input data for the minimum volume problem was prepared as required by the formulation of the primary discrete setting $(\hat{P}_1)$, while the dual approach $(\hat{P}_2)$ was automatically defined, and solved, by MOSEK through a built-in routine. For the convenience of the reader, in Fig. 3 we present the flow chart of MATLAB procedures for solving $(\hat{P}_1)$, and $(\hat{P}_2)$.

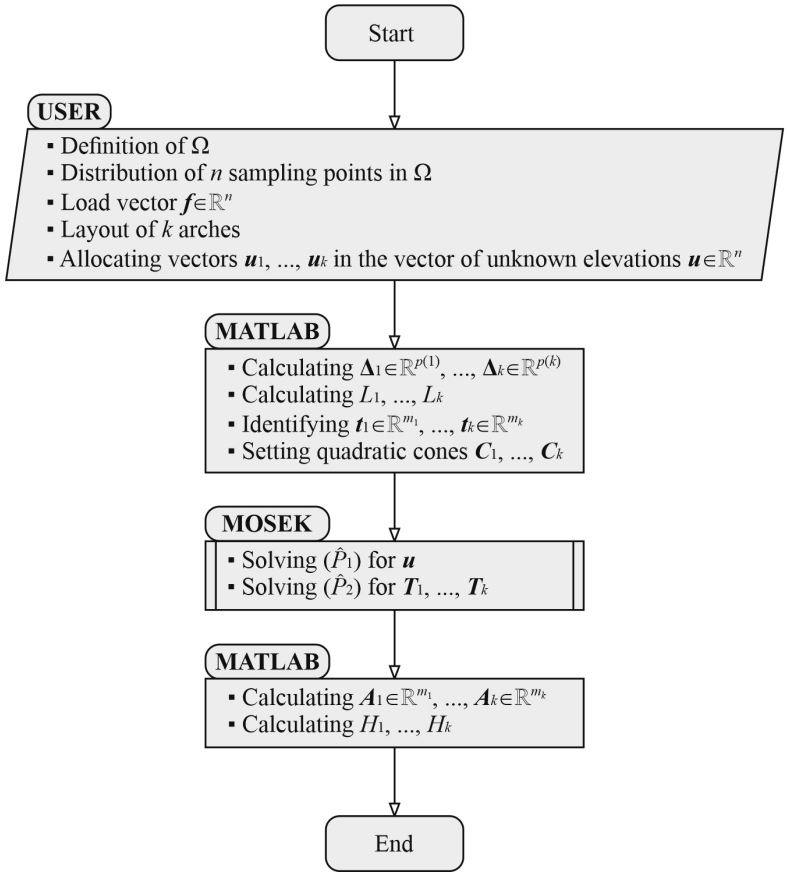

Fig. 3. The flow chart of numerical procedures in MATLAB and MOSEK. Symbols used in the chart coincide with those in Sec. 2. We emphasize that MOSEK is a third-party, add-on toolbox of routines for conic optimization

3.1. Example 1: square domain

In this example, we consider the $\Omega = [0, 2L] \times [0, 2L]$ square domain and two load cases:

- q = const. acting above the entire Ω (load case 1), see Fig. 4;
- q = const. acting above the middle part $[0.5L, 1.5L] \times [0.5L, 1.5L] \subset \Omega$ (load case 2), see Fig. 5.

Results obtained with help of the SOCP approach put forward in this paper are compared with the conclusions from the study in [5], where the minimum volume problem was solved in the continuous setting; see Table 1 for the collected results. More precisely, the elevation function v has been approximated in terms of the Fourier (trigonometric) and Legendre (polynomial)

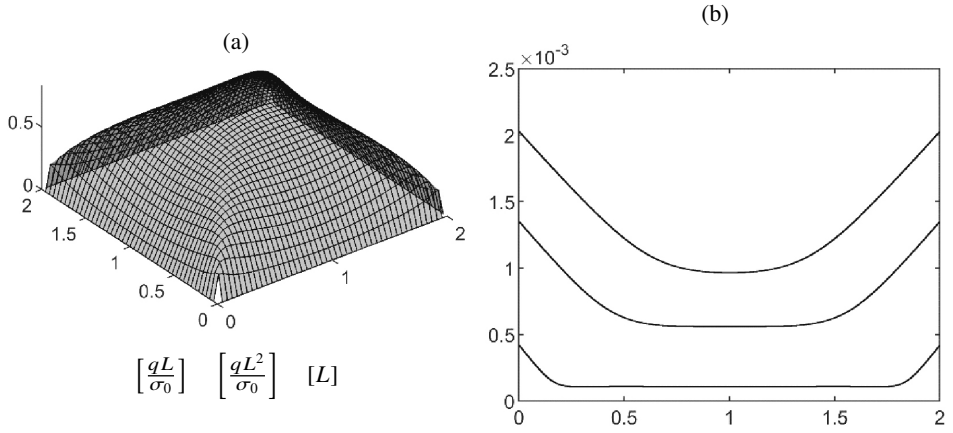

Fig. 4. a) Optimal archgrid elevation function v for load case 1 in Example 1, b) optimal cross-section area functions for arches at $x = 0.2L$ (bottom line), $x = 0.6L$ (middle line), and $x = L$ (top line)

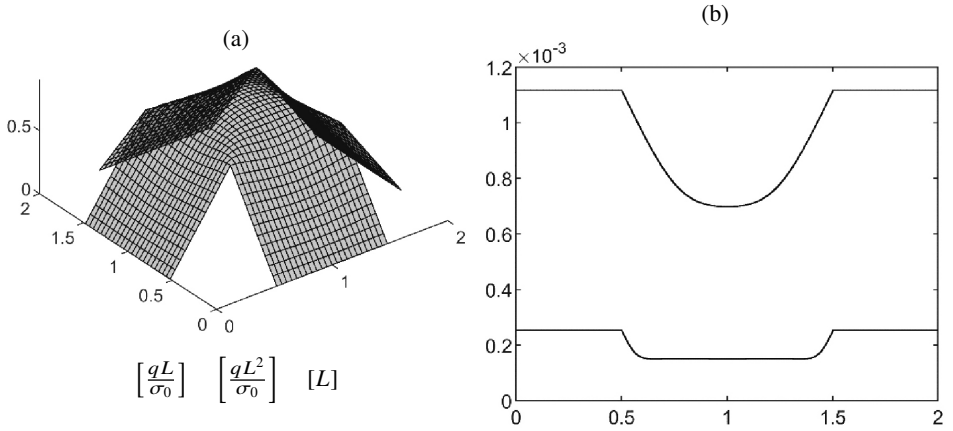

Fig. 5. a) Optimal archgrid elevation function v for load case 2 in Example 1, b) optimal cross-section area functions for arches at $x = 0.2L$ (bottom line, $A_{\text{opt}} = 0$), $x = 0.6L$ (middle line), and $x = L$ (top line)

series in the orthogonal coordinates. For this reason, the comparison of results is limited to the orthogonal layout of arches.

Table 1. Square domain Ω with q = const. above the entire domain (load case 1) and q = const. above the middle part of the domain (load case 2). Comparison of results obtained for different numerical approaches

load case	number of arches along x and y arch orientations with respect to x	discrete approach with SOCP, [this paper]		continuous approach with Fourier approximation, [4]		continuous approach with Legendre approximation, [4]	
		CPU time	optimal volume	CPU time	optimal volume	CPU time	optimal volume
1	45×45 arches $0°$ and $90°$	0.5 sec	$3.677\frac{qL^3}{\sigma_0}$	131 sec	$3.681\frac{qL^3}{\sigma_0}$	167 sec	$3.681\frac{qL^3}{\sigma_0}$
1	100×100 arches $0°$ and $90°$	1.7 sec	$3.680\frac{qL^3}{\sigma_0}$	4784 sec	$3.681\frac{qL^3}{\sigma_0}$	9063 sec	$3.681\frac{qL^3}{\sigma_0}$
1	1000×1000 arches $0°$ and $90°$	216 sec	$3.681\frac{qL^3}{\sigma_0}$	out of memory	–	out of memory	–
2	45×45 arches $0°$ and $90°$	0.6 sec	$1.560\frac{qL^3}{\sigma_0}$	500 sec	$1.561\frac{qL^3}{\sigma_0}$	1319 sec	$1.561\frac{qL^3}{\sigma_0}$
2	100×100 arches $0°$ and $90°$	2 sec	$1.560\frac{qL^3}{\sigma_0}$	12458 sec	$1.561\frac{qL^3}{\sigma_0}$	53442 sec	$1.561\frac{qL^3}{\sigma_0}$
2	1000×1000 arches $0°$ and $90°$	182 sec	$1.561\frac{qL^3}{\sigma_0}$	out of memory	–	out of memory	–

3.2. Example 2: circular domain

In this example, we consider the $\Omega = [0,\ R] \times [0,\ 2\pi]$ circular domain and three load cases:

- q = const. acting above the entire Ω (load case 1);
- q = const. acting above the middle part $[0,\ 0.5R] \times [0,\ 2\pi] \subset \Omega$ (load case 2);
- point load $Q = qR^2$ acting above the center of Ω (load case 3).

Potential directions of arches for the problem $(\hat{P}_1)$ are arbitrary. However, only radial arches are optimal, i.e. satisfy the mean squared slope condition. Plots in Fig. 6a) show the meridian lines of optimal elevation functions related to each load case in Example 2, while the plot in Fig. 6b) shows the layout of optimal arches in load case 1. Analytical solution for the latter case,

$$V_{\text{opt}} = \frac{2\pi}{\sqrt{5}} \frac{qR^3}{\sigma_0} \tag{3.1}$$

was obtained in [1] through the purely mathematically approach via the measure theory. In Table 1, we compare (3.1) with suboptimal results obtained by the SOCP.

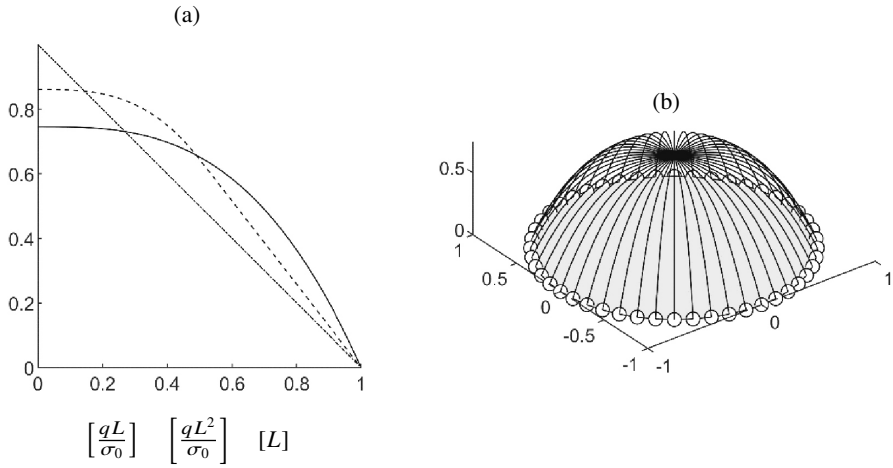

Fig. 6. a) Optimal meridian lines in Example 2: load case 1 (solid line), load case 2 (dashed line), load case 3 (dash-dotted line), b) scheme of optimal layout of arches in load case 1

Table 2. Circular domain Ω with q = const. above the entire domain (load case 1). Comparison of V_{opt} in (3.1) with realistic suboptimal results, V_{SOCP} obtained by SOCP

load case	number of radial arches spanning Ω	discrete approach with SOCP	
		V_{SOCP}	$V_{\text{SOCP}}/V_{\text{opt}} - 1$
1	18 arches	$2.995\dfrac{qR^3}{\sigma_0}$	6.59%
1	36 arches	$2.905\dfrac{qR^3}{\sigma_0}$	3.38%
1	72 arches	$2.858\dfrac{qR^3}{\sigma_0}$	1.71%

4. Conclusions

Variational approach to the Rozvany–Prager problem of spanning a given domain with an k-element archgrid of minimum weight (equivalently, minimum volume) involves two, mutually dual formulations. The complete solution includes a scalar field v representing the archgrid elevation function and a k-component vector field $(Q_1, \ldots, Q_k)$ having a clear mechanical interpretation following from the equilibrium equations for single arches. In the discrete approach, these fields are respectively replaced by $\boldsymbol{u}$ and $(\boldsymbol{T}_1, \ldots, \boldsymbol{T}_k)$. Specific mathematical features of the discrete optimization problem allows for reinterpreting it from the second-order cone programming (SOCP) point of view. Such a line of action turns out to be extremely robust in terms of the CPU time, if compared to the continuous approach based on the Fourier or Legendre series. The robustness of the computational algorithm manifests itself also in its capability to make a clear-cut distinction between optimal and non-optimal parts of the structure. The latter

are redundant from engineer's point of view as they do not carry any load, see Example 1, load case 2. Optimal archgrid consists only in these members for which the mean squared slope equals 1. Adding new arches, or removing any of the existing ones, would result in member force redistribution and reshaping of the entire archgrid. As a consequence, the volume of a structure would increase.

Acknowledgement

This paper was prepared with financial support from the Research Grant no 2019/33/B/ST8/00325 financed by the National Science Centre (Poland), entitled: *Merging the optimum design problems of structural topology and of the optimal choice of material characteristics. The theoretical foundations and numerical methods.*

References

[1] K. Bołbotowski, "Optimal vault problem – form finding through 2D convex program". Preprint published at arxiv.org. https://arxiv.org/abs/2104.07148.

[2] S. Boyd and L. Vandenberghe, "Convex optimization". Cambridge University Press, Cambridge: UK, 2004.

[3] R. Czubacki, G. Dzierżanowski, and T. Lewiński, "Obliczenia numeryczne przekryć Pragera". Inżynieria i Budownictwo, vol. 1–2, pp. 80–84, Jan.-Feb. 2021. (in Polish).

[4] R. Czubacki and T. Lewiński, "Optimal archgrids: a variational setting". Structural and Multidisciplinary Optimization, vol. 62, pp. 1371–1393, Sep. 2020, DOI: 10.1007/s00158-020-02562-y.

[5] G. Dzierżanowski and R. Czubacki, "Optimal archgrids spanning rectangular domains". Computers and Structures, vol. 242, article 106371, Jan 2021, DOI: 10.1016/j.compstruc.2020.106371.

[6] L. He and M. Gilbert, "Rationalization of trusses generated via layout optimization". Structural and Multidisciplinary Optimization, vol. 52, pp. 677–694, Oct. 2015, DOI: 10.1007/s00158-015-1260-x.

[7] W.S. Hemp, "Optimum structures". Clarendon Press, Oxford: UK, 1973.

[8] K. Hetmański and T. Lewiński, "Kształtowanie ram i łuków płaskich niepodlegających zginaniu". in Theoretical Foundations of Civil Engineering. Polish-Ukrainian-Lithuanian Transactions, vol. 15, W. Szcześniak, ed. Warsaw: Warsaw University of Technology Publishing House (in Polish).

[9] T. Lewiński, T. Sokół, and C. Graczykowski, "Michell structures, Springer Nature". Cham: Switzerland, 2019.

[10] G.I.N. Rozvany, H. Nakamura and B.T. Kuhnell, "Optimal archgrids: allowance for selfweight". Computer Methods in Applied Mechanics and Engineering, vol. 24, pp. 287–304, Dec. 1980, DOI: 10.1016/0045-7825(80)90066-3.

[11] G.I.N. Rozvany and W. Prager, "A new class of structural optimization problems: optimal archgrids". Computer Methods in Applied Mechanics and Engineering, vol. 19, pp. 127–150, Jun. 1979, DOI: 10.1016/0045-7825(79)90038-0.

[12] G.I.N. Rozvany and C.M. Wang, "On plane Prager-structures – I". International Journal of Mechanical Sciences, vol. 25, pp. 519–527, 1983, DOI: 10.1016/0020-7403(83)90044-9.

[13] G.I.N. Rozvany, C.M. Wang, and M. Dow, "Prager-structures: archgrids and cable networks of optimal layout". Computer Methods in Applied Mechanics and Engineering, vol. 31, pp. 91–113, Jul. 1982, DOI: 10.1016/0045-7825(82)90049-4.

[14] C. Smith, et al., "Application of layout optimization to the design of additively manufactured metallic components". Structural and Multidisciplinary Optimization, vol. 54, pp. 1297–1313, April 2016, DOI: 10.1007/s00158-016-1426-1.

[15] T. Sokół, "A 99 line code for discretized Michell truss optimization written in Mathematica". Structural and Multidisciplinary Optimization, vol. 43, pp. 181–190, Feb. 2011, DOI: 10.1007/s00158-010-0557-z.

[16] V. Thevendran and C.M. Wang, "On the optimality criteria for archgrids". Journal of Structural Engineering, vol. 112, pp. 185–189, Jan. 1986, DOI: 10.1061/(ASCE)0733-9445(1986)112:1(185).

[17] C.M. Wang and G.I.N. Rozvany, "On plane Prager-structures – II. Non-parallel loads and allowances for selfweight". International Journal of Mechanical Sciences, vol. 25, pp. 529–541, 1983, DOI: 10.1016/0020-7403(83)90045-0.

[18] Website: https://www.mathworks.com/ (accessed on 8.06.2021).

[19] Website: https://www.mosek.com/ (accessed on 8.06.2021).

Optymalne kształtowanie siatek łukowych w ujęciu programowania stożkowego drugiego stopnia

Słowa kluczowe: konstrukcje o minimalnej objętości, optymalne siatki łukowe, siatki Rozvany'ego–Pragera, programowanie stożkowe

Streszczenie:

Praca dotyczy projektowania siatek łukowych ze względu na minimum ciężaru (albo, równoważnie, minimum objętości) materiału użytego do ich konstrukcji. Tematyka została wprowadzona do literatury naukowej przez G.I.N. Rozvany'ego i W. Pragera w latach 70-tych XX wieku, kiedy autorzy sformułowali zadanie kształtowania najlżejszej, rozpiętej nad danym obszarem płaskim, konstrukcji łukowej zdolnej przenieść obciążenie o danej intensywności do linii podpór znajdującej się na brzegu obszaru. Forma architektoniczna przekrycia przybiera postać siatki oddalonych od siebie łuków podpartych przegubowo na obu końcach. Co za tym idzie, z mechanicznego punktu widzenia, zadanie statyki kopuły jest rozważane w ramach teorii powłok siatkowych, a nie powłok o budowie ciągłej.

Zadanie minimum objętości siatek łukowych należy do szerokiego nurtu zagadnień topologicznej optymalizacji konstrukcji. Ściślej, *siatki łukowe Rozvany'ego–Pragera* są szczególnym przykładem *konstrukcji Pragera*, które z kolei należą do ogólnej kategorii *konstrukcji Michella*. Cechy różniące wspomniane koncepcje projektowania optymalnego najłatwiej wskazać posługując się *kryterium pełnego wytężenia konstrukcji*. W rozumieniu tego kryterium, konstrukcja prętowa jest optymalna w sensie Michella, jeżeli w każdym jej punkcie stan naprężenia odpowiada granicy sprężystości przy ściskaniu, σ_C, bądź rozciąganiu, $-\sigma_T$ (w pracy przyjęto konwencję dodatniego znakowania naprężeń ściskających). Taka sytuacja jest możliwa jedynie wtedy, gdy pręty układu nie podlegają zginaniu i ścinaniu, a działające na układ obciążenie zewnętrzne jest w całości przejmowane przez siły osiowe w prętach. W przypadku konstrukcji Pragera i siatek łukowych Rozvany'ego–Pragera zakłada się dodatkowo, że naprężenia w całej konstrukcji przybierają wartości tego samego znaku – tzn. są wyłącznie ściskające, bądź rozciągające. W pracy rozważamy zadanie konstrukcji z prętów ściskanych, zakładając tym samym $\sigma_C = \sigma_0 > 0$ oraz $\sigma_T = 0$.

Kryterium pełnego wytężenia odnosi się do pojedynczych prętów, a więc algorytmy komputerowe oparte o to kryterium pozwalają na znalezienie ram optymalnych w sensie Michella i Pragera. Projektowanie siatek łukowych Rozvany'ego–Pragera wymaga innego podejścia, w którym miejsce pojedynczego pręta zajmuje łuk płaski, przybierający w ujęciu dyskretnym kształt linii łamanej, złożonej z wielu prętów prostych i podpartej przegubowo na obu końcach. Z tego względu, kryterium pełnego wytężenia wymaga przeformułowania do postaci uwzględniającej budowę takiego elementu łukowego. W rezultacie, dostosowanie algorytmów numerycznych zorientowanych na projektowanie konstrukcji Michella do potrzeb wynikających ze specyfiki siatek łukowych Rozvany'ego–Pragera nie jest intuicyjne.

Celem pracy było opracowanie algorytmu numerycznego optymalizacji w sensie Rozvany'ego–Pragera w ujęciu programowania stożkowego drugiego stopnia. W tym celu wykorzystano możliwości środowiska MATLAB wzbogaconego o pakiet bibliotek optymalizacyjnych MOSEK. Proponowane nowe

spojrzenie na zadanie minimum objętości pozwoliło na zapisanie procedur obliczeniowych znacznie szybszych, niż stosowane dotychczas, co z kolei umożliwiło analizę konstrukcji złożonych z bardzo dużej liczby prętów (rzędu $\sim 10^6$). Otrzymane wyniki wykraczają poza potrzeby przemysłu konstrukcji inżynierskich, ale znacząco wspomagają rozważania teoretyczne zagadnień optymalizacji w ujęciu ciągłym.

W pracy korzystamy z następujących oznaczeń: Ω – określa przekrywany obszar parametryzowany współrzędnymi (x, y); Γ – linię podpór znajdującą się na brzegu Ω; v – powierzchnię nad Ω, na której leżą osie łuków; n – liczbę węzłów w zbiorze $\Omega \cup \Gamma$, w których wyznacza się wyniosłość powierzchni v; $\boldsymbol{u} \in \mathbb{R}^n$ – wektor wyniosłości; $\boldsymbol{f} \in \mathbb{R}^n$ – wektor obciążeń działających prostopadle do Ω; k – liczbę łuków siatki; L_K – rozpiętość K-tego łuku ($K = 1, \ldots, k$); $\boldsymbol{t}_K = \boldsymbol{B}_K \boldsymbol{u}$, gdzie $\boldsymbol{B}_K$ jest daną macierzą – wektor tangensów kąta nachylenia prętów K-tego łuku względem Ω. Ze względu na kierunek działania obciążenia zakładamy, że osie łuków leżą w płaszczyznach prostopadłych do Ω i dowolnie zorientowanych względem układu (x, y). Dodatkowo, wprowadzamy oznaczenie

$$\boldsymbol{C}_K = \left\{ \left(\sqrt{L_K}, \boldsymbol{B}_K \boldsymbol{u} \right) \mid \|\boldsymbol{B}_K \boldsymbol{u}\|_2 \leq \sqrt{L_K} \right\}$$

na określenie K-tego stożka drugiego stopnia, przy czym $\|\cdot\|_2$ jest normą euklidesową wektora. Formuła

$$\|\boldsymbol{B}_K \boldsymbol{u}\|_2 = \sqrt{L_K}$$

nosząca w literaturze nazwę *warunku średniokwadratowego nachylenia*, zastępuje kryterium pełnego wytężenia.

Zadanie optymalizacji siatek łukowych Rozvany'ego–Pragera przybiera dwie postaci – pierwotną i dualną. W realizacji numerycznej zadania programowane jest zadanie pierwotne, tj. zadanie maksymalizacji pracy obciążenia zewnętrznego po kinematycznie dopuszczalnych wektorach wyniosłości – tzw. zmiennych pierwotnych:

$$\left| \begin{array}{l} \hat{Z}_1 = \max \left\{ \boldsymbol{f}^T \boldsymbol{u} \mid \boldsymbol{u} \in U \right\} \\ \text{gdzie:} \\ \mathcal{U} = \boldsymbol{u} \left\{ \begin{array}{l} \boldsymbol{u} \in \mathbb{R}^n \ \text{ oraz } \ u_K = 0 \ \text{ jeżeli } N\text{-ty węzeł znajduje siię na } \Gamma \\ \left(\sqrt{L_k}, \boldsymbol{B}_K \boldsymbol{u} \right) \in \boldsymbol{C}, \ \text{ dla kazdego } K = 1, \ldots, k \end{array} \right\} \end{array} \right.$$

natomiast zadanie dualne jest formułowane i rozwiązywane automatycznie w procedurze pakietu MOSEK. W wyniku rozwiązania zadania pierwotnego otrzymuje się optymalny wektor $\boldsymbol{u}_{\text{opt}}$, pozwalający obliczyć optymalną objętość siatki

$$V_{\text{opt}} = \frac{2}{\sigma_0} \boldsymbol{f}^T \boldsymbol{u}_{\text{opt}},$$

zaś rozwiązanie zadania dualnego określa optymalne wartości zmiennych dualnych $(\boldsymbol{T}_{1,\text{opt}} \ldots, \boldsymbol{T}_{K,\text{opt}})$, na podstawie których oblicza się optymalne pola przekroju poprzecznego prętów tworzących łuki siatki. Zmienne dualne są związane z wektorem obciążenia wzorem

$$\sum_{K=1}^{k} (\boldsymbol{B}_K)^T \boldsymbol{T}_{K,\text{opt}} = \boldsymbol{f}.$$

Received: 2021-05-04, Revised: 2021-06-13